

High-Spin Polyphenoxy Based on Poly(1,4-phenyleneethynylene)

Hiroyuki Nishide,* Tadatoshi Maeda, Kenichi Oyaizu, and Eishun Tsuchida

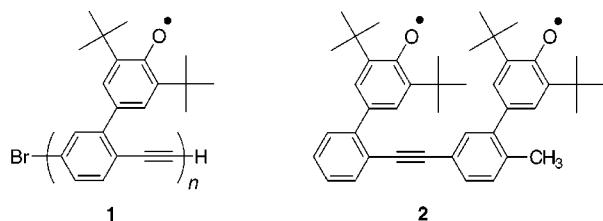
Department of Polymer Chemistry, Waseda University, Tokyo 169-8555, Japan

Received April 23, 1999

Rodlike poly(1,4-phenyleneethynylene) 2-substituted with multiple pendant phenoxy radicals **1** was synthesized by polymerizing 4-bromo-2-(3,5-di-*tert*-butyl-4-hydroxyphenyl)ethynylbenzene **10a** using the catalyst of a palladium–triphenylphosphine complex and cuprous iodide and subsequent heterogeneous oxidation. The corresponding dimer **2** was also synthesized; X-ray analysis of its precursor **4** indicated a linear phenyleneethynylene backbone and twisted dihedral angles of 50 and 77° for the pendant phenol groups. ESR spectra suggested a delocalized spin distribution from the pendant phenoxy to the backbone. The diphenoxyl **2** had a triplet ($S = 2/2$) ground state. The spin concentration of the polyphenoxy **1** could not be increased beyond 0.7 spin/unit due to its low solvent solubility; **1** with a spin concentration of 0.62 had an average S of 3/2.

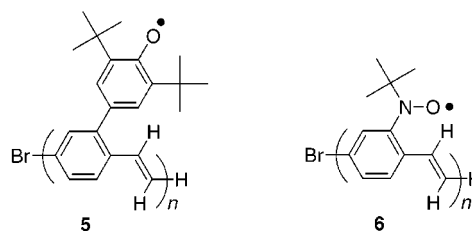
Introduction

One of the potential candidates to produce a very high-spin and purely organic-derived molecule is a π -conjugated polymer bearing multiple pendant radical groups, which are attached to one π -conjugated backbone that satisfies non-Kekulé structures and the non-disjoint connectivity of nonbonding molecular orbitals (NBMOs).^{1,2} The π -conjugated backbone acts as a ferromagnetic coupler to align the pendant radical's spins based on an intrapolymer and through-bond spin-exchange interaction. We have synthesized the pendant polyradicals based



on poly(phenylenevinylene)s, such as poly[2-(3,5-di-*tert*-butyl-4-oxyphenyl)-1,4-phenylenevinylene] (**5**),³ poly[4-(3,5-di-*tert*-butyl-4-oxyphenyl)-1,2-phenylenevinylene],⁴ and poly[2-(*N*-*tert*-butyl-*N*-oxyamino)-1,4-phenylenevinylene] (**6**),⁵ and succeeded in realizing a through-conjugated backbone and long-range ferromagnetic exchange inter-

action between the pendant unpaired electrons. Poly(phenylenevinylene) possesses coplanarity and an extended π -conjugation length even after substitution on the phenylene ring. However, our computational study⁴ suggested for the poly(1,4-phenylenevinylene)-based polyphenoxy a highly twisted dihedral angle (ca. 70°) of the pendant phenoxy group toward the relatively coplanar backbone. The source of strain appeared to be the proximity of the pendant phenoxy group to the ethylenic C–H bond in **5**. On the other hand, the radical (spin) concentration could not be increased for **6** because of intramolecular side reactions; every pendant *tert*-butyl-nitroxide group was a neighbor to the hydrogen of the vinylene bridge in **6**.



An ethynylene bridge is characterized by a sterically compact and hydrogen-free structure. It involves two orthogonal π -bonds. Poly(phenyleneethynylene) looks like a favorable choice as a π -conjugated and ferromagnetically coupling backbone of the polyradicals, which are sterically crowded and often chemically unstable and whose conjugations suffer considerable twisting. Miura et al. have already synthesized poly(1,3(*meta*)-phenyleneethynylene)-based polyradicals such as poly[5-(nitronyl nitroxide- or *tert*-butyl nitroxide-substituted)-1,3-phenyleneethynylene].⁶ While this poly[5-(radical-substituted)-1,3-phenyleneethynylene] does not involve the problem of a structural regularity in the head-to-tail linkage due to its symmetric substitutions on the phenylene ring, the connectivity of its substitution positions of radicals is of the disjoint type^{1d,7} in the π -conjugation or its NBMOs

(1) For reviews on high-spin organic molecules, see: (a) Iwamura, H.; Koga, N. *Acc. Chem. Res.* **1993**, *26*, 346. (b) Rajca, A. *Chem. Rev.* **1994**, *94*, 871. (c) Nishide, H. *Adv. Mater.* **1995**, *7*, 937. (d) Lahti, P. M. *Magnetic Properties of Organic Materials*; Marcel Dekker: New York, 1998.

(2) For recent papers on very high-spin organic molecules, see: (a) Rajca, A.; Lu, K.; Rajca, S. *J. Am. Chem. Soc.* **1997**, *119*, 10355. (b) Rajca, A.; Wongstriratanakul, J.; Rajca, S. *J. Am. Chem. Soc.* **1997**, *119*, 11674. (c) Ruiz-Molina, D.; Veciana, J.; Palacio, F.; Rovira, C. *J. Org. Chem.* **1997**, *62*, 2, 9009. (d) Rajca, A.; Wongstriratanakul, J.; Rajca, S.; Cerny, R. *Angew. Chem., Int. Ed. Engl.* **1998**, *37*, 1229. (e) Bushby, R.; Gooding, D. *J. Chem. Soc., Perkin Trans. 2*, **1998**, 1069. (f) Nishide, H.; Miyasaka, M.; Tsuchida, E. *Angew. Chem., Int. Ed. Engl.* **1998**, *37*, 2400. (g) Nishide, H.; Miyasaka, M.; Tsuchida, E. *J. Org. Chem.* **1998**, *63*, 7399.

(3) Nishide, H.; Kaneko, T.; Nii, T.; Katoh, K.; Tsuchida, E.; Yamaguchi, K. *J. Am. Chem. Soc.* **1995**, *117*, 548.

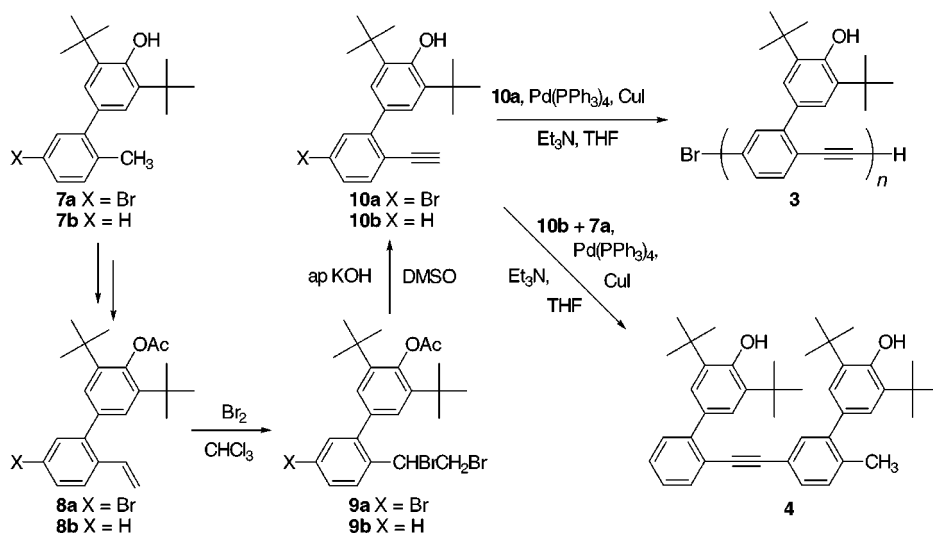
(4) Nishide, H.; Kaneko, T.; Nii, T.; Katoh, K.; Tsuchida, E.; Lahti, P. M. *J. Am. Chem. Soc.* **1996**, *118*, 9695.

(5) Nishide, H.; Kaneko, T.; Toriu, S.; Kuzumaki, Y.; Tsuchida, E. *Bull. Chem. Soc. Jpn.* **1996**, *69*, 499.

(6) (a) Miura, Y.; Matsumoto, M.; Ushitani, Y.; Teki, Y.; Itoh, K. *Macromolecules*, **1993**, *26*, 6673. (b) Miura, Y.; Issiki, T.; Ushitani, Y.; Teki, Y.; Itoh, K. *J. Mater. Chem.* **1996**, *6*, 1745.

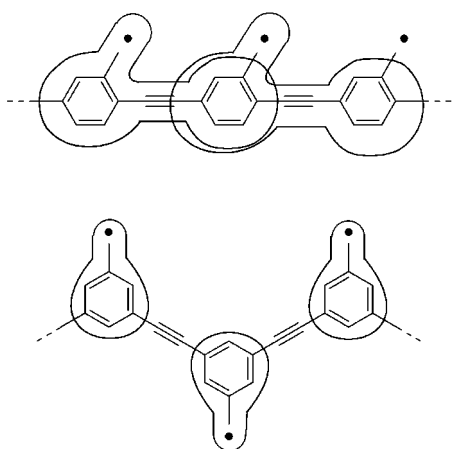
(7) Borden, W. T.; Davison, E. R. *J. Am. Chem. Soc.* **1977**, *99*, 4587.

Scheme 1



are confined to separate regions in the molecule to minimize the spin-exchange interaction (as schematically represented in Chart 1). The real poly(1,3-phenylene-

Chart 1



ethynylene)-based polyradicals displayed only paramagnetic or weak antiferromagnetic behavior.⁶

On the other hand, a poly[2-(radical substituted)-1,4-(*para*)-phenyleneethynylene] is characterized by a non-disjoint connectivity (Chart 1), and its NBMOs share the same molecular region that enhances the ferromagnetic spin-exchange interaction. Although poly(1,4-phenyleneethynylene)s have usually been synthesized via the condensation of *p*-diethynylbenzene and *p*-dihalogenobenzene,⁸ these lack the restricted primary structure of a head-to-tail linkage for the monosubstituted poly(1,4-phenyleneethynylene) formation. A complete head-to-tail linkage of the monomer unit is the first requisite for a ferromagnetic high-spin alignment, since a synthetic error such as a head-to-head linkage in the polymer backbone cancels out the high-spin alignment. In this paper, we report the first synthesis of a poly(1,4-phenyleneethynylene) bearing pendantly 2-substituted phenoxyl radicals and discuss its structure and high-spin

state by comparison to those of the corresponding diphenoxyl compound.

Results and Discussion

Synthesis of the Poly- and Diphenol Precursors.

The monomer of the polyphenol precursor, 4-bromo-2-(3,5-di-*tert*-butyl-4-hydroxyphenyl)ethynylbenzene **10a**, was synthesized from 4-bromo-2-(3,5-di-*tert*-butyl-4-hydroxyphenyl)toluene **7a**, as shown in Scheme 1. **7a** was protected with an acetoxy group, and the methyl group was modified to a vinyl group via the Wittig reaction to yield **8a**. The vinyl group of **8a** was converted to an ethynyl group via the addition of bromine and the subsequent elimination of hydrogen bromide with a strong base to give **10a**. **10a** was polymerized in THF via a cross-coupling reaction using the catalyst of a palladium-triphenylphosphine complex and cuprous iodide to yield the polymer **3**. Polymerization of the trimethylsiloxy-protected **10a** resulted in a similar yield and molecular weight, thus negating any poisoning effect of the catalyst by the phenolic hydroxy group. The polymer was insoluble in common solvents except for THF. The molecular weight of the product polymer depended on its solubility in the polymerization solvent. The polymer with a molecular weight of 3.6×10^3 (degree of polymerization or n in **3** = 11) was precipitated during the polymerization even in THF.

As the precursor of a diphenoxyl analogue **2**, 3,2'-bis-(3,5-di-*tert*-butyl-4-hydroxyphenyl)-4-methyldiphenylacetylene **4** was synthesized by the cross-coupling of 2-(3,5-di-*tert*-butyl-4-hydroxyphenyl)ethynylbenzene **10b** and 4-bromo-2-(3,5-di-*tert*-butyl-4-hydroxyphenyl)toluene **7a** in the presence of the Pd(PPh₃)₄-CuI catalyst (Scheme 1).

Structure of the Poly- and Diphenols. The precursor phenols, **10a** and **4**, were isolated as colorless prism-like crystals. The crystal structures were determined on the basis of an X-ray crystallographic analysis (Figure 1). The structure of the monomer phenol **10a** had a dihedral angle of 37° between the phenol group and the phenylene ring (Figure 1a). For the diphenol compound **4** (Figure 1b), the dihedral angle between the two phenylene rings linked with the ethynylene bridge was 12°, which indicates an approximately linear and copla-

(8) (a) Trumbo, D. L.; Marvel, C. S. *J. Polym. Sci., Polym. Chem. Ed.* **1986**, *24*, 2311. (b) Bochmann, M.; Kelly, K. *J. Chem. Soc., Chem. Commun.* **1989**, 532.

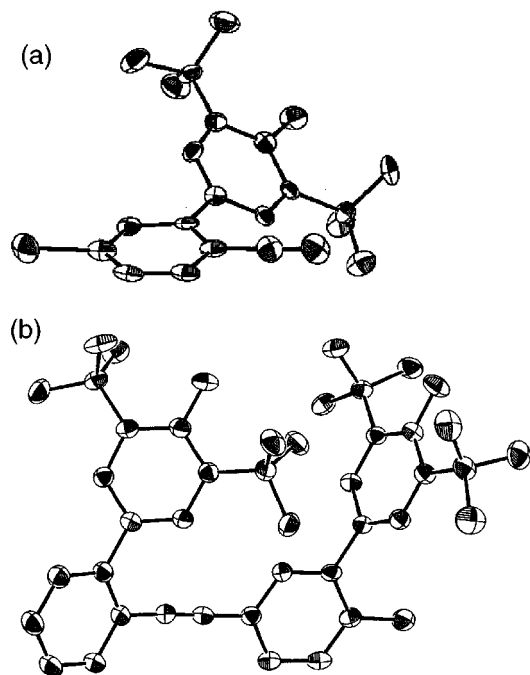


Figure 1. ORTEP views of the phenol **10a** (a) and the diphenol **4** (b).

nar 1,4-phenyleneethynylene backbone. Due to possible rotation of the 1,4-phenylene group, the neighboring pair of pendant phenol groups may either be syn or anti to one another. Interestingly, the syn conformer is found to be more stable than the anti conformer in the X-ray structure. The dihedral angles between the pendant phenol groups and the phenylene rings were 50 and 77°.

Calculations were carried out using the CVFF force field for **10a** and **4**. The full geometry optimization suggested that the dihedral angles between the phenol groups and the phenyleneethynylene backbone were 50°, and 58 and 62° for **10a** and **4**, respectively. These angles are comparable with those determined in the crystal structures. The syn conformer was also preferred in the calculation of the diphenol **4**. The computational study on the pentaphenol ($n = 5$ in **3**) suggested an *all-syn* and rodlike conformer with the dihedral angle of ca. 50° between any pendant phenol group and the phenyleneethynylene backbone.

The UV-vis absorption and fluorescence spectra of the polyphenol precursor in dilute THF solutions are shown in Figure 2. The absorption is shifted to longer wavelengths from the monophenol **10b**, to the diphenol **4**, and to the polyphenol **3**. This bathochromic shift is attributed to an extension of the π -conjugation. Under UV irradiation, the polyphenol **3** fluoresces a blue color, which is ascribed to a diphenylethynylene moiety. The emission spectrum ($\lambda_{\text{ex}} = 375$ nm) of the THF solution of **3** is also given in Figure 2. While this fluorescence intensity at $\lambda_{\text{em}} = 435$ nm was proportional to the **3** concentration for the dilute solution, it significantly decreased beyond ca. 25 mg/L (inset of Figure 2). It was considered that the rodlike polymer **3** aggregates at the higher concentration to quench the fluorescence. This was supported by the apparent increase in molecular weight up to 1.8×10^4 for the concentrated (50 mg/L) solution of **3** with a true molecular weight of 2.4×10^3 and by the turbidity increase for the solution beyond 0.1 g/L.

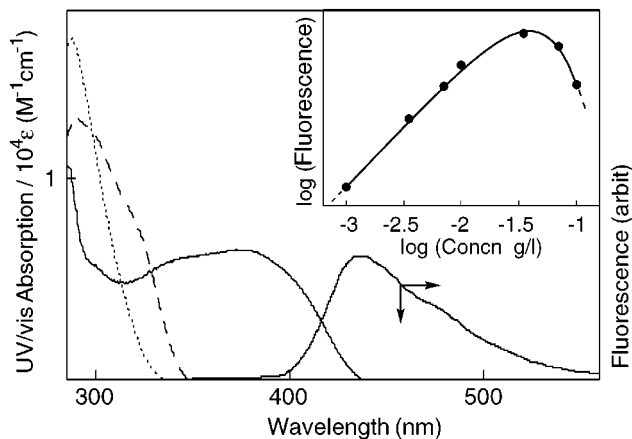


Figure 2. UV-vis absorption spectra of the polyphenol precursor **3** (—), the diphenol precursor **4** (---) and the monophenol precursor **10a** (···) and the fluorescence spectrum ($\lambda_{\text{ex}} = 375$ nm) of the polyphenol precursor **3** (—) in dilute THF solutions. Inset: Fluorescence intensity of **3** at 435 nm vs concentration of **3** in the THF solution.

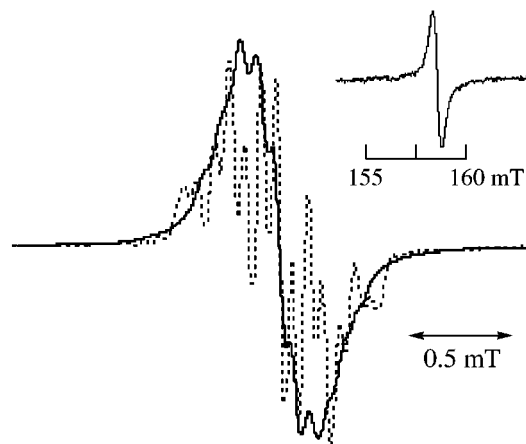


Figure 3. ESR spectra of the polyphenoxy **1** with spin concn = 0.08 spin/unit (—) in 2-methyl-THF at $g = 2.0041$ and of the monophenoxy of **10a** with spin concn = 0.12 (---) in toluene at $g = 2.0042$ at room temperature. Inset: $\Delta M_s = \pm 2$ spectrum of **1** with spin concn = 0.62.

Magnetic Properties of Poly- and Diphenoxyls.

The phenol precursors (**3** and **4**) were converted to deeply red-colored phenolate anions with a small excess of tetra-*n*-butylammonium hydroxide in THF and then heterogeneously treated with an aqueous ferricyanide solution to yield the phenoxy radicals (**1** and **2**). GPC elution curves of the polymers before and after the radical generation (**3** and **1**) coincided with each other, which denied oxidative scission or cross-linking of the polymer backbone. However, the poly(1,4-phenyleneethynylene)-based polyphenoxy **1** was chemically not very stable as expected; e.g., the half-life of the radical estimated by the following ESR signal intensity was 5.6 h in a THF solution at room temperature and rather shorter than that for the poly(1,4-phenylenevinylene)-based **5** (7.2 h) under the same conditions.

Figure 3 shows the ESR spectrum of **1** with a low spin concentration; the broad but hyperfine spectrum was ascribed to the protons of the pendant phenoxy and the backbone phenylene rings. The dashed line in Figure 3 shows the hyperfine spectrum of the monoradical of **10a**, which indicates an interaction with at least four kinds

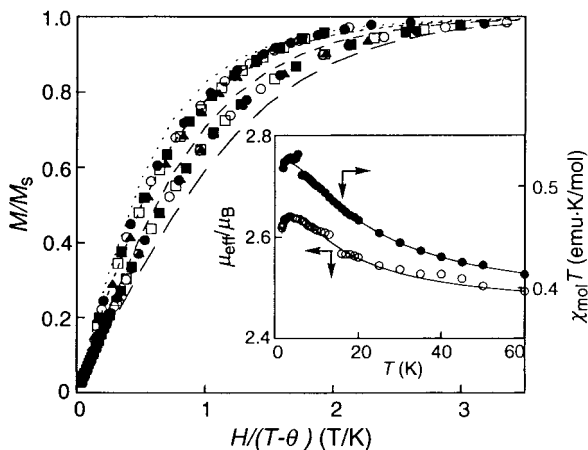


Figure 4. Normalized plots of magnetization (M/M_s) vs the ratio of magnetic field and temperature ($H/(T - \theta)$) for the polyphenoxyl **1** with spin concn = 0.62 spin/unit and the diphenoxyl **2** with spin concn = 0.69 in frozen 2-methyl-THF at $T = 1.8$ (●), 2.0 (○), 2.25 (■), 2.5 (□), 3.0 (▲), and 5.0 (△) K, and the theoretical curves corresponding to the 1/2, 2/2, 3/2, and 4/2 Brillouin functions. Inset: $\chi_{\text{mol}}T$ vs T plots of the polyphenoxyl **1** (●) and μ_{eff}/μ_B vs T plots of the diphenoxyl **2** (○). Solid lines are theoretical curves calculated using van Vleck expression for **1** with spin concn = 0.36 ($2J = 18 \text{ cm}^{-1}$, $\theta = -0.01 \text{ K}$, $x_1 = 0.02$, $x_2 = 0.28$, $x_3 = 0.70$) and the modified Bleaney–Bowers expression for **2** with spin concn = 0.69 ($2J = 12 \text{ cm}^{-1}$, $\theta = -0.09 \text{ K}$, $x_1 = 0.4$, $x_2 = 0.6$).

of proton. These results suggest a delocalized spin distribution from the pendant phenoxy to the phenyleneethynylene backbone.

With increasing spin concentration, the ESR spectrum of **1** gave a sharp and unimodal signal at $g = 2.0041$ assigned to an oxygen-centered radical. The inset in Figure 3 shows a $\Delta M_s = \pm 2$ forbidden transition ascribed to a triplet species at $g = 4$ for **1** with a spin concentration of 0.62 spin/monomer unit. Although this signal intensity was proportional to the reciprocal of temperature according to the Curie law at higher temperature, the intensity deviated upward from the linearity in the low temperature (<15 K) region. This upward deviation supported a multiplet ground state for the polyphenoxyl **1**.

The magnetization and static magnetic susceptibility of the diphenoxyl radical **2** and the polyphenoxyl radical **1** in frozen 2-methyl-THF were measured using a SQUID magnetometer to estimate the intramolecular spin coupling through the phenyleneethynylene backbone between the pendant phenoxy radicals. The magnetization (M) normalized with saturated magnetization (M_s) for **2** is plotted vs the effective temperature ($T - \theta$) (Figure 4), where θ is the coefficient of a weak and through-space antiferromagnetic interaction between radicals and is determined from curve fitting using the following magnetic susceptibility data. The M/M_s plots for **2** were found to lie close to the Brillouin curve for $S = 2/2$ at low temperature, indicating a triplet ground state for the diphenoxyl radical **2**.

The ratio of the effective magnetic moment (μ_{eff}) and the Bohr magneton (μ_B), μ_{eff}/μ_B , was calculated from the magnetic susceptibility and the spin concentration, and the plots of μ_{eff}/μ_B vs T for the diphenoxyl radical **2** are shown in the inset of Figure 4. The plots lie close to the $\mu_{\text{eff}}/\mu_B = 2.45$ at higher temperature and to 2.83 at low temperature, which are theoretical values for $S = 1/2$ and 2/2, respectively. The Bleaney–Bowers equation has been

modified for the analysis of the μ_{eff}/μ_B data for incomplete spin generation samples of diradicals and expressed by the sum of the complete diradical fraction (x_2) and the doublet monoradical fraction (x_1).⁹ The spin-exchange coupling constant (J) of the intramolecular spin-alignment was estimated for **2** by curve fitting the μ_{eff}/μ_B vs T data to the modified Bleaney–Bowers equation. The resulting parameters are summarized in the caption of Figure 4. The $2J$ or stability of the triplet ground state (ΔE_{T-S}) value was estimated to be 12 cm^{-1} for **2**. This positive $2J$ value indicates a through-bond or intramolecular ferromagnetic coupling, but it was smaller than that of the corresponding 1,2-phenyleneethynylene isomer, 3,4'-bis(3,5-di-*tert*-butyl-4-oxyphenyl)diphenylacetylene ($2J = 31 \text{ cm}^{-1}$).¹⁰ The reduced spin-exchange interaction is considered to be caused by twisting of the pendant phenoxy groups toward the phenyleneethynylene backbone (for its phenol precursor, the dihedral angles of 50 and 77° in Figure 1).

The M/M_s plots for **1** with a spin concentration of 0.62 lie almost on the Brillouin curve for $S = 3/2$ at low temperature (Figure 4), indicating a ferromagnetic spin-coupling, on the average, between the three pendant phenoxy radicals. The product of the molar magnetic susceptibility (χ_{mol}) and T for **1** increases at low temperature, as shown in the inset of Figure 4. J was estimated by curve fitting the $\chi_{\text{mol}}T$ data to the equation derived from the van Vleck expression¹¹ for a linear three-spin model. $2J = 18 \text{ cm}^{-1}$ for **1** was somewhat larger than that for the diradical **2** ($2J = 12 \text{ cm}^{-1}$).

These results concluded that the π -conjugated poly-(1,4-phenyleneethynylene) backbone was not a very strong ferromagnetic coupler as expected because it took the all-syn conformation and the pendant phenoxy groups were still twisted toward the backbone despite the sterically compact and hydrogen-free ethynylene bridge. However, the poly(1,4-phenyleneethynylene) backbone ferromagnetically coupled the pendant spins and displayed $S = 3/2$, which was the highest in comparison with the magnetic data previously reported for the poly(phenyleneethynylene)-based polyradicals.^{6,10} The S value was reasonable by taking into account both the degree of polymerization of **11** and the spin defect of ca. 40% for the polyphenoxyl **1**, which were caused by the low solvent solubility of **1**. After optimization of the radical generation step, the poly(1,4-phenyleneethynylene) still could be a candidate for an effective backbone of the pendant-type and high-spin polyradicals because its rodlike structure would bring about one of the secondary functions, such as liquid crystal formation, besides the molecular-based magnetic property.

Experimental Section

4-Bromo-2-(3,5-di-*tert*-butyl-4-hydroxyphenyl)ethynylbenzene (10a). 4-Bromo-2-(3,5-di-*tert*-butyl-4-acetoxyphenyl)-styrene **8a** was prepared as has been reported in our previous

(9) $\mu_{\text{eff}}/\mu_B = [6g^2T(1 - x_1)(T - \theta)^{-1}\{3 + \exp(-2J/kT)\}^{-1} + 3g^2Tx_1\{2(T - \theta)\}^{-1}]^{1/2}$. Bleaney, B.; Bowers, K. D. *Proc. R. Soc. London* **1952**, *A214*, 451.

(10) Nishide, H.; Takahashi, M.; Takashima, J.; Pu, Y.-J.; Tsuchida, E. *J. Org. Chem.*, in press.

(11) $\chi_{\text{mol}}T = N_A g^2 \mu_B^2 T [k(T - \theta)]^{-1} \{ [x_2/12] [1 + \exp(-2J/kT)] + 10 \exp(-J/kT) [1 + \exp(-2J/kT)] + 2 \exp(J/kT) \}^{-1} + x_2 [3 + \exp(-2J/kT)]^{-1} + x_1/4$, where x_1 , x_2 , and x_3 are the fraction of the doublet, the triplet, and the quartet, respectively ($x_1 + x_2 + x_3 = 1$). Vleck, J. H. V. *The Theory of Electric and Magnetic Susceptibilities*; Oxford University Press: London, 1932.

paper.⁴ A chloroform solution (41 mL) of **8a** (20.7 g, 48.2 mmol) was cooled to 0 °C, and a chloroform solution of bromine (7.7 g, 48.4 mmol) was slowly added and stirred for 30 min at room temperature. After being washed with saturated aqueous sodium sulfite, the organic layer was extracted with chloroform, washed with water, dried over anhydrous sodium sulfate, and evaporated. Recrystallization from chloroform afforded 27.9 g (98%) of the product **9a** as a colorless solid. Without further purification, **9a** (1.7 g, 2.9 mmol) was dissolved in a small amount of DMSO. A 70% aqueous sodium hydroxide solution (2 mL) was added dropwise to the solution and was stirred for 5 h at 50 °C. The mixture was neutralized with aqueous ammonium chloride, extracted with diethyl ether, washed with water, dried over sodium sulfate, and evaporated. The crude product was purified by column chromatography on silica gel with a chloroform/hexane (1/12) eluent. Recrystallization from hexane gave **10a** (0.30 g) as colorless crystals: yield 27%; mp 141 °C; IR (KBr pellet, cm⁻¹) 3625 ($\nu_{\text{O-H}}$), 3283 ($\nu_{\text{C-H}}$), 2953 ($\nu_{\text{C-H}}$), 2085 ($\nu_{\text{C=C}}$); ¹H NMR (CDCl₃, 500 MHz, ppm) 1.46 (s, 18H), 3.12 (s, 1H), 5.31 (s, 1H), 7.37–7.54 (m, 5H); ¹³C NMR (CDCl₃, ppm) 30.4, 34.5, 80.7, 83.0, 119.1, 123.1, 126.0, 129.2, 129.6, 132.3, 135.3, 135.4, 146.9, 154.0; mass calcd for M 385.3, found (*m/z*) 384, 386 (M⁺). Anal. Calcd for C₂₂H₂₅BrO: C, 68.6; H, 6.5; Br, 20.8. Found: C, 68.6; H, 6.8; Br, 20.8.

Polymerization. A THF solution (21 mL) of **10a** (801 mg, 2.1 mmol), tetrakis(triphenylphosphine)palladium(0) (240 mg, 0.21 mmol), cuprous iodide (80 mg, 0.42 mmol), and triethylamine (4.2 g, 42 mmol) was refluxed for 20 h under nitrogen. The solution was treated with dilute hydrochloric acid, extracted with chloroform, washed with water, dried over sodium sulfate, and evaporated. The product was purified by reprecipitation from hot THF into methanol to give the polymer as a yellow powder (270 mg): yield 34%; IR (KBr pellet, cm⁻¹) 3635 ($\nu_{\text{O-H}}$), 2957 ($\nu_{\text{C-H}}$), 2203 ($\nu_{\text{C=C}}$); ¹H NMR (THF-*d*₆, 500 MHz, ppm) 1.43 (s, 18H), 6.32 (s, 1H), 7.23–7.73 (m, 5H); molecular weight (measured by a light-scattering molecular weight analyzer Tosoh LS-8000) 3.6×10^3 (DP = 11), *M_w/M_n* = 1.3. Anal. Calcd for C_{22*n*}H_{24*n*+1}BrO_{*n*} (*n* = 11): C, 84.8; H, 7.8; Br, 2.3. Found: C, 84.9; H, 7.6; Br, 2.2.

3,2'-(3,5-Di-*tert*-butyl-4-hydroxyphenyl)-4-methyldi-phenylacetylene (4). 2-(3,5-Di-*tert*-butyl-4-hydroxyphenyl)-ethynylbenzene **10b** was prepared by bromination of the vinyl group of 2-(3,5-di-*tert*-butyl-4-acetoxyphenyl)styrene **8b**⁴ and the following dehydrobromination under strong alkaline conditions, as described for **10a**: yield 40%; IR (KBr pellet, cm⁻¹) 3633 ($\nu_{\text{O-H}}$), 3307 ($\nu_{\text{C-H}}$), 2965 ($\nu_{\text{C-H}}$), 2100 ($\nu_{\text{C=C}}$); ¹H NMR (CDCl₃, 500 MHz, ppm) 1.48 (s, 18H), 3.08 (s, 1H), 5.27 (s, 1H), 7.24–7.61 (m, 6H); ¹³C NMR (CDCl₃, ppm) 30.4, 34.5, 79.8, 84.0, 119.7, 122.1, 126.2, 129.0, 129.4, 130.5, 134.1, 135.2, 145.1, 153.6; mass calcd for M 306, found (*m/z*) 306 (M⁺). Anal. Calcd for C₂₂H₂₆O: C, 86.3; H, 8.5. Found: C, 86.3; H, 8.6.

A THF solution (33 mL) of **10b** (3.3 mmol), 4-bromo-2-(3,5-di-*tert*-butyl-4-hydroxyphenyl)toluene **7a** (3.3 mmol), cuprous iodide (0.33 mmol), tetrakis(triphenylphosphine)palladium(0) (0.17 mmol), and triethylamine (66 mmol) was refluxed for 20 h under nitrogen. The solution was treated with dilute hydrochloric acid, extracted with chloroform, washed with water, evaporated, and purified using a silica gel column with a chloroform/hexane (1/4) eluent. Recrystallization from hexane afforded **4** (0.61 g) as colorless crystals: yield 31%; mp 204 °C; IR (KBr pellet, cm⁻¹) 3639 ($\nu_{\text{O-H}}$), 2957 ($\nu_{\text{C-H}}$), 2210 ($\nu_{\text{C=C}}$); ¹H NMR (CDCl₃, 500 MHz, ppm) 1.43, 1.45 (s, 36H), 2.26 (s, 3H), 5.19, 5.21 (s, 2H), 7.04–7.63 (m, 11H); ¹³C NMR (CDCl₃, ppm) 20.7, 30.4, 34.4, 89.3, 92.1, 120.8, 121.5, 125.6, 126.1, 126.2, 128.2, 129.5, 129.6, 130.2, 131.6, 132.1, 133.0, 133.2, 135.2, 135.4, 135.9, 142.9, 144.5, 152.8, 153.4; mass calcd for M 600.9, found (*m/z*) 601 (M⁺). Anal. Calcd for C₄₃H₅₂O₂: C, 86.0; H, 8.7. Found: C, 85.6; H, 8.6.

Oxidation. Aqueous solutions of sodium hydroxide and potassium ferricyanide (10 and 20 equiv to the phenol group, respectively) were successively added to a 2-methyl-THF solution (1–20 mmol/L) of the hydroxy precursor (**3** or **4**) with vigorous stirring at room temperature in a glovebox. The mixture turned to deep green after 5 min. After the mixture

was stirred for 30 min, the organic layer was separated, washed with water, and dried over anhydrous sodium sulfate to give the radical solution.

ESR and SQUID Measurements. ESR spectra were taken using a JEOL TE-200 ESR spectrometer with a 100 kHz field modulation. The spin concentration of each sample was determined both by careful integration of the ESR signal standardized with that of 2,2,6,6-tetramethyl-1-piperidinyloxy solution and by analyzing the saturated magnetization at the SQUID measurement.

The 2-methyl-THF solution of radical was immediately transferred to a diamagnetic capsule after the oxidation. Magnetization and static magnetic susceptibility were measured with a Quantum Design MPMS-7 SQUID magnetometer. The magnetization was measured from 0 to 7 T at 1.8, 2, 2.25, 3, 5, 10, 15, and 20 K. The static magnetic susceptibility was measured from 1.8 to 200 K at a field of 0.5 T.

Other Spectroscopic Measurements. The ¹H and ¹³C NMR, MS, FAB-MS, UV-vis, IR, and fluorescence spectra were measured using a JEOL Lambda 500 or a JNM-EX270, a Shimadzu GCMS-QP5050, a JMS-SX 102A, a JASCO V-500, a JASCO FTIR 410, and a Hitachi F-4500 spectrometer, respectively.

X-ray Crystallography. Colorless prismatic crystals of **10a** and **4** were grown from their hexane solutions. Following microscopic examination in air, a suitable crystal was mounted on a glass fiber at room temperature. All measurements were made on a Rigaku AFC7R diffractometer with a 6.0 kW rotating anode generator and graphite monochromated MoK α radiation ($\lambda = 0.71073$ Å). Unit cell parameters and an orientation matrix for data collection were determined by least-squares refinements using the setting angles of 25 carefully centered reflections in the range of $15.11 < 2\theta < 17.70^\circ$ for **10a** and of $29.73 < 2\theta < 29.97^\circ$ for **4**. The data were collected at 25 °C using the $\omega - 2\theta$ scan technique to a maximum 2θ value of 55° . The intensities of three representative reflections were measured after every 150 reflections. No decay correction was applied. An empirical absorption correction based on the azimuthal scans of several reflections was applied that resulted in transmission factors ranging from 0.70 to 1.00 for **10a** and from 0.83 to 1.00 for **4**. The data were corrected for Lorentz and polarization effects. A correction for secondary extinction was also applied (coefficient: **10a**, 9.7014×10^{-7} ; **4**, 1.12402×10^{-6}).

Structure Solution and Refinement. The structure was solved by heavy-atom Patterson methods and expanded using Fourier techniques. The positions for most non-hydrogen atoms were visible on the initial *E*-map with positions of the remaining atoms found on subsequent electron density difference maps. The non-hydrogen atoms were anisotropically refined. Hydrogen atoms were included but not refined. The final cycle of full-matrix least-squares refinement¹² was based on 1306 observed reflections ($I > 3\sigma(I)$) and 275 variable parameters for **10a** and 4915 observed reflections and 434 variable parameters for **4**. Crystal data for **10a**: space group *P*2₁ (#4), *a* = 6.37(2) Å, *b* = 16.954(7) Å, *c* = 9.30(2) Å, $\beta = 98.5(3)^\circ$, *V* = 993(4) Å³, *Z* = 2, *D*_{calc} = 1.288 g/cm³, μ (Mo K α) = 20.79 cm⁻¹, final $R = \sum ||F_o| - |F_c|| / \sum |F_o| = 0.058$ and $R_w = (\sum w(|F_o| - |F_c|)^2 / \sum w F_o^2)^{1/2} = 0.029$. Crystal data for **4**: space group *P*1 (#2), *a* = 13.563(2) Å, *b* = 14.220(2) Å, *c* = 10.177(1) Å, $\alpha = 101.00(1)^\circ$, $\beta = 90.94(1)^\circ$, $\gamma = 84.95(1)^\circ$, *V* = 1919.2(5) Å³, *Z* = 2, *D*_{calc} = 1.119 g/cm³, μ (Mo K α) = 0.68 cm⁻¹, final $R = \sum ||F_o| - |F_c|| / \sum |F_o| = 0.087$ and $R_w = (\sum w(|F_o| - |F_c|)^2 / \sum w F_o^2)^{1/2} = 0.078$. The plots of $\sum w(|F_o| - |F_c|)^2$ versus $|F_o|$, reflection order in the data collection, $\sin \theta/\lambda$ and various classes of indices showed no unusual trends. All calculations were performed using the teXsan crystallographic software package of Molecular Structure Corporation.¹³

Computational Methods. The CVFF-optimized conformations were obtained by repeated energy minimization and

(12) Least-squares: Function minimized: $\sum w(|F_o| - |F_c|)^2$, where $w = (\sigma(F_o)^2 + (0.020(F_o))^2)^{-1}$.

(13) teXsan: Crystal Structure Analysis Package, Molecular Structure Corp., 1985 and 1992.

annealing dynamics calculations (100–5000 K) using the Discover program from Molecular Simulations Inc. The X-ray structural data were employed as the initial structural parameters for the simulation. The molecular dynamics simulations were carried out with the initial velocities randomly assigned in order to realize the Boltzmann distribution at each temperature.

Acknowledgment. This work was partially supported by a Grant-in-Aid for Scientific Research (No.

09305060) from the Ministry of Education, Science, Sports and Culture, Japan, and by the NEDO Project on Technology for Novel High-Functional Materials.

Supporting Information Available: Tables giving atomic coordinates, anisotropic displacement parameters, bond lengths and bond angles of **10a** and **4**. This material is available free of charge via the Internet at <http://pubs.acs.org>.

JO990691L